Chapter 8

New Results in DF Relaying Schemes Using Time Diversity for Free-Space Optical Links

Rubén Boluda-Ruiz, Beatriz Castillo-Vázquez,
Carmen Castillo-Vázquez and
Antonio García-Zambrana

Additional information is available at the end of the chapter

http://dx.doi.org/10.5772/58996

1. Introduction

Atmospheric free-space optical (FSO) transmission using intensity modulation and direct detection (IM/DD) can be considered as an important alternative to consider for next generation broadband in order to support large bandwidth, unlicensed spectrum, excellent security, and quick and inexpensive setup [1]. Nonetheless, this technology is not without drawbacks, being the atmospheric turbulence one of the most impairments, producing fluctuations in the irradiance of the transmitted optical beam, which is known as *atmospheric scintillation*, severely degrading the link performance [2]. Additionally, since FSO systems are usually installed on high buildings, building sway causes vibrations in the transmitted beam, leading to an unsuitable alignment between transmitter and receiver and, hence, a greater deterioration in performance. Error control coding as well as diversity techniques can be used over FSO links to mitigate turbulence-induced fading [3–6]. In [7], the effects of atmospheric turbulence and misalignment considering aperture average effect were considered to study the outage capacity for single-input/single-output (SISO) links. In [8, 9], a wide range of turbulence conditions with gamma-gamma atmospheric turbulence and pointing errors is also considered on terrestrial FSO links, deriving closed-form expressions for the error-rate performance in terms of Meijer's G-functions. In [10, 11], comparing different diversity techniques, a significant improvement in terms of outage and error-rate performance is demonstrated when multiple-input/multiple-output (MIMO) FSO links based on transmit laser selection are adopted in the context of wide range of turbulence conditions with pointing errors. An alternative approach to provide spatial diversity in this turbulence FSO scenario without using multiple lasers and apertures is the employment of cooperative communications. Cooperative transmission can significantly improve the performance by creating diversity using the transceivers available at the other nodes of the network. This is a well known technique employed in radio-frequency (RF) systems, wherein more attention has been paid to the concept of user cooperation as a new form of diversity for future wireless communication systems [12]. Recently, several works have investigated the adoption of this technique in the context of FSO systems [13–19], being recognized as a very promising solution for future ad-hoc optical wireless systems. In [14, 15] a 3-way FSO communication setup is proposed to implement a cooperative protocol in order to improve spatial diversity without much increase in hardware, being evaluated the error-rate performance by using the photon-count method as well as the outage performance for both amplify-and-forward (AF) and decode-and-forward (DF) strategies. In [19], following the bit-detect-and-forward (BDF) cooperative protocol presented in [14], the analysis is extended to FSO communication systems using IM/DD over atmospheric turbulence and misalignment fading channels, considering cooperative communications with BDF relaying and equal gain combining (EGC) reception. In contrast to the BDF strategy considered in [14], it is assumed in [19] in addition to the analysis of the impact of pointing errors that all the bits detected at the relay are always resended regardless of these bits are detected correctly or incorrectly. Next, bits received directly from the source and from the relay are detected at destination node following an EGC technique. In [20], a novel BDF relaying scheme based on repetition coding with the relay and EGC is proposed, improving the robustness to impairments proper to these systems such as unsuitable alignment between transmitter and receiver as well as fluctuations in the irradiance of the transmitted optical beam due to the atmospheric turbulence, compared to the BDF relaying scheme analyzed in [19].

In this chapter, a novel closed-form approximation bit error-rate (BER) expression based on [21] is presented for a 3-way FSO communication setup when the irradiance of the transmitted optical beam is susceptible to either a wide range of turbulence conditions (weak to strong), following a gamma-gamma distribution of parameters α and β, or pointing errors, following a misalignment fading model where the effect of beam width, detector size and jitter variance is considered. The resulting BER expression is shown to be very accurate in the range from low to high SNR, requiring the first two terms of the Taylor expansion of the channel probability density function (PDF). Simulation results are further demonstrated to confirm the accuracy and usefulness of the derived results. The superiority of the BDF relaying scheme using time diversity, compared with the cooperative protocol in [19], is corroborated by the obtained results since a greater robustness is provided not only to the pointing errors but also to the relay location, presenting a similar performance regardless of the source-destination link distance.

2. System and channel model

As shown in Fig. 1, we adopt a three-node cooperative system based on three separate full-duplex FSO links, assuming laser sources intensity-modulated and ideal noncoherent (direct-detection) receivers. For this 3-way FSO communication setup the cooperative protocol can be applied to achieve the spatial diversity without much increase in hardware. The BDF cooperative protocol here proposed is based on the use of repetition coding in the transmission corresponding to the source-relay link, fully exploiting a time diversity order of 2 in the atmospheric channel in a similar approach to [22]. As shown in Table 1, the cooperative strategy works in three phases or transmission frames. In the first phase, the nodes A and B send their own data to each other and the destination node C, i.e., the node A (B) transmits the same information to the nodes B (A) and C. In the second transmission frame, the nodes A and B send again the same information to each other delayed

http://dx.doi.org/10.5772/58996

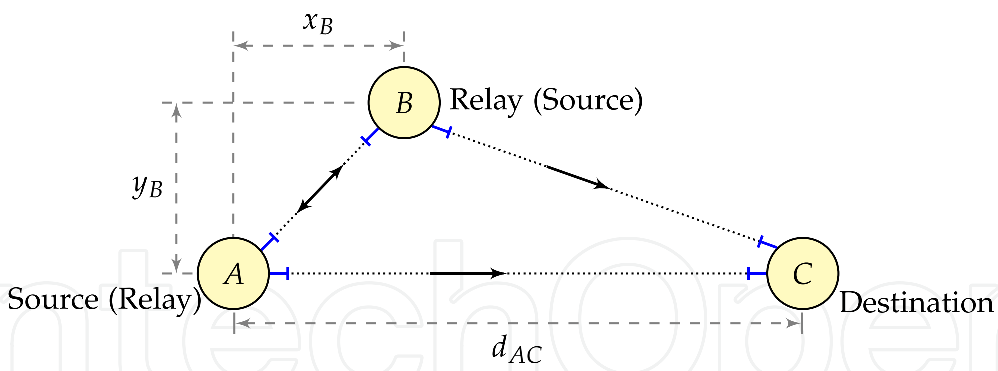

Figure 1. Block diagram of the considered 3-way FSO communication system, where d_{AC} is the A-C link distance and (x_B, y_B) represents the location of the node B.

by the expected fade duration and, hence, assuming that channel fades are independent and identically distributed (i.i.d.). In the third phase, the node B (or A) sends the received data from its partner A (or B) in previous frames to the node C. Following the BDF cooperative protocol, the relay node (A or B) detects each code bit to "0" or "1" based on repetion coding and sends the bit with the new power to the destination node C. When repetition coding is used in the source-relay link transmission during the first and second phases, the information is detected each transmission frame, combining with the same weight two noisy faded signals in a similar manner to a single-input multiple-output (SIMO) FSO scheme with EGC [23] and, this way, achieving a diversity gain of 2 for this link.

Symbol	t_1	t_2	t_3	$\cdots$	t_n	t_{n+1}	t_{n+2}	t_{n+3}
$A \to C$								
1	$A \to B$ $A \to C$			$\cdots$	$A \to B$	$B \to C$		
2		$A \to B$ $A \to C$		$\cdots$		$A \to B$	$B \to C$	
3			$A \to B$ $A \to C$	$\cdots$			$A \to B$	$B \to C$
$\vdots$								
$B \to C$								
1	$B \to A$ $B \to C$			$\cdots$	$B \to A$	$A \to C$		
2		$B \to A$ $B \to C$		$\cdots$		$B \to A$	$A \to C$	
3			$B \to A$ $B \to C$	$\cdots$			$B \to A$	$A \to C$
$\vdots$								

Table 1. BDF cooperative scheme based on repetition coding in the source-relay link transmission.

It must be noted that the symmetry for nodes A and B assumed in this FSO communication setup and the fact that one transmission frame is overlapped imply that no rate reduction is applied, i.e., the same information rate can be considered at the destination node C compared to the direct transmission link without using any cooperative strategy. As in [19], it is assumed in this paper that all the bits detected at the relay are always resended regardless of these bits are detected correctly or incorrectly. Next, bits received directly from A-C and from the relay A-B-C are detected at C following an EGC technique. Since atmospheric scintillation is a slow time varying process relative to typical symbol rates of an FSO system, having a coherence time on the order of milliseconds, we consider the time variations according to the theoretical block-fading model, where the channel fade remains constant during a block (corresponding to the channel coherence interval) and changes to a new independent value from one block to next. In other words, channel fades are assumed to be independent and identically distributed. This temporal correlation can be overcome by means of long interleavers, being usually assumed both in the analysis from the point of view of information theory and error rate performance analysis of coded FSO links [4, 5, 24]. However, as in [22, 25], we here assume that the interleaver depth can not be infinite and, hence, we can potentially benefit from a degree of time diversity limited equal to 2. This consideration is justified from the fact that the latency introduced by the interleaver is not an inconvenience for the required application. In the cooperative protocol here proposed, wherein repetition coding and a time diversity order available of 2 is assumed in the source-relay link transmission, perfect interleaving can be done by simply sending the same information delayed by the expected fade duration, as shown experimentally in [26].

For each link of the three possible links in this three-node cooperative FSO system, the instantaneous current $y_m(t)$ in the receiving photodetector corresponding to the information signal transmitted from the laser can be written as

$$y_m(t) = \eta i_m(t)x(t) + z(t) \tag{1}$$

where η is the detector responsivity, assumed hereinafter to be the unity, $X \triangleq x(t)$ represents the optical power supplied by the source and $I_m \triangleq i_m(t)$ the equivalent real-valued fading gain (irradiance) through the optical channel between the laser and the receive aperture. Additionally, the fading experienced between source-detector pairs I_m is assumed to be statistically independent. $Z \triangleq z(t)$ is assumed to include any front-end receiver thermal noise as well as shot noise caused by ambient light much stronger than the desired signal at the detector. In this case, the noise can usually be modeled to high accuracy as AWGN with zero mean and variance $\sigma^2 = N_0/2$, i.e. $Z \sim N(0, N_0/2)$, independent of the on/off state of the received bit. Since the transmitted signal is an intensity, X must satisfy $\forall t\, x(t) \geq 0$. Due to eye and skin safety regulations, the average optical power is limited and, hence, the average amplitude of X is limited. The received electrical signal $Y_m \triangleq y_m(t)$, however, can assume negative amplitude values. We use Y_m, X, I_m and Z to denote random variables and $y_m(t)$, $x(t)$, $i_m(t)$ and $z(t)$ their corresponding realizations.

The irradiance is considered to be a product of three factors i.e., $I_m = \zeta_m I_m^{(a)} I_m^{(p)}$ where ζ_m is the deterministic propagation loss, $I_m^{(a)}$ is the attenuation due to atmospheric turbulence and $I_m^{(p)}$ the attenuation due to geometric spread and pointing errors. ζ_m is determined by the exponential Beers-Lambert law as $\zeta_m = e^{-\Phi d}$, where d is the link distance and Φ is the atmospheric attenuation coefficient. It is given by $\Phi = (3.91/V(km))\,(\lambda(nm)/550)^{-q}$ where V is the visibility in kilometers, λ is the wavelength in nanometers and q is the size distribution of the scattering particles, being $q = 1.3$ for average visibility (6 km $< V <$ 50 km), and $q = 0.16V + 0.34$ for haze visibility (1 km $< V <$ 6 km)

[27]. To consider a wide range of turbulence conditions, the gamma-gamma turbulence model proposed in [2] is here assumed. Regarding to the impact of pointing errors, we use the general model of misalignment fading given in [7] by Farid and Hranilovic, wherein the effect of beam width, detector size and jitter variance is considered. A closed-form expression of the combined probability density function (PDF) of I_m was derived in [8] as

$$f_{I_m}(i) = \frac{\alpha_m \beta_m \varphi_m^2}{A_0 \zeta_m \Gamma(\alpha_m)\Gamma(\beta_m)} G_{1,3}^{3,0}\left(\frac{\alpha_m \beta_m}{A_0 \zeta_m} i \,\middle|\, \begin{matrix} \varphi_m^2 \\ \varphi_m^2 - 1, \alpha_m - 1, \beta_m - 1 \end{matrix} \right), \quad i \geq 0 \tag{2}$$

where $G_{p,q}^{m,n}[\cdot]$ is the Meijer's G-function [28, eqn. (9.301)] and $\Gamma(\cdot)$ is the well-known Gamma function. Assuming plane wave propagation, α and β can be directly linked to physical parameters through the following expresions [29]:

$$\alpha = \left[\exp\left(0.49\sigma_R^2 / (1 + 1.11\sigma_R^{12/5})^{7/6} \right) - 1 \right]^{-1} \tag{3a}$$

$$\beta = \left[\exp\left(0.51\sigma_R^2 / (1 + 0.69\sigma_R^{12/5})^{5/6} \right) - 1 \right]^{-1} \tag{3b}$$

where $\sigma_R^2 = 1.23 C_n^2 \kappa^{7/6} d^{11/6}$ is the Rytov variance, which is a measure of optical turbulence strength. Here, $\kappa = 2\pi/\lambda$ is the optical wave number and d is the link distance in meters. C_n^2 stands for the altitude-dependent index of the refractive structure parameter and varies from $10^{-13}\ m^{-2/3}$ for strong turbulence to $10^{-17}\ m^{-2/3}$ for weak turbulence [2]. It must be emphasized that parameters α and β cannot be arbitrarily chosen in FSO applications, being related through the Rytov variance. It can be shown that the relationship $\alpha > \beta$ always holds, and the parameter β is lower bounded above 1 as the Rytov variance approaches ∞ [30]. In relation to the impact of pointing errors [7], assuming a Gaussian spatial intensity profile of beam waist radius, ω_z, on the receiver plane at distance z from the transmitter and a circular receive aperture of radius r, $\varphi = \omega_{z_{eq}}/2\sigma_s$ is the ratio between the equivalent beam radius at the receiver and the pointing error displacement standard deviation (jitter) at the receiver, $\omega_{z_{eq}}^2 = \omega_z^2 \sqrt{\pi}\mathrm{erf}(v)/2v\exp(-v^2)$, $v = \sqrt{\pi}r/\sqrt{2}\omega_z$, $A_0 = [\mathrm{erf}(v)]^2$ and $\mathrm{erf}(\cdot)$ is the error function [28, eqn. (8.250)]. Nonetheless, the PDF in Eq. (2) appears to be cumbersome to use in order to obtain simple closed-form expressions in the analysis of FSO communication systems. To overcome this inconvenience, the PDF is approximated by using the first two terms of the Taylor expansion at $i = 0$ as $f_{I_m}(i) = a_m i^{b_m - 1} + c_m i^{b_m} + O(i^{b_m+1})$. As proposed in [21], we adopt the approximation $f_{I_m}(i) \approx a_m i^{b_m - 1} \exp(i c_m / a_m)$. Different expressions for $f_{I_m}(i)$, depending on the relation between the values of φ^2 and β, can be written as

$$f_{I_m}(i) \approx \frac{\varphi_m^2 (\alpha_m \beta_m)^{\beta_m} \Gamma(\alpha_m - \beta_m)}{(A_0 \zeta_m)^{\beta_m} \Gamma(\alpha_m)\Gamma(\beta_m)\left(\varphi_m^2 - \beta_m\right)} i^{\beta_m - 1} e^{i \frac{\alpha_m \beta_m \left(\varphi_m^2 - \beta_m\right)}{A_0 \zeta (\alpha_m - \beta_m - 1)\left(\beta_m - \varphi_m^2 + 1\right)}}, \qquad \varphi_m^2 > \beta_m \tag{4a}$$

$$f_{I_m}(i) \approx \frac{\varphi_m^2 (\alpha_m \beta_m)^{\varphi_m^2} \Gamma\left(\alpha_m - \varphi_m^2\right) \Gamma\left(\beta_m - \varphi_m^2\right)}{(A_0 \zeta_m)^{\varphi_m^2} \Gamma(\alpha_m)\Gamma(\beta_m)} i^{\varphi_m^2 - 1}, \qquad \varphi_m^2 < \beta_m \tag{4b}$$

It can be noted that the second term of the Taylor expansion is equal to 0 when the diversity order is not independent of the pointing error effects, i.e. $\varphi_m^2 < \beta_m$. In the following section, the fading coefficient I_m for the paths A-B, A-C and and B-C is indicated by I_{AB}, I_{AC} and I_{BC}, respectively.

3. Error-rate performance analysis

For the sake of clarity, without loss of generality, we can consider node A as source and node B as its relay for the BER evaluation since similar results hold when node B is considered as the source and node A as its relay. In addition to the BER performance evaluation corresponding to the cooperative protocol here proposed based on time diversity, we also consider the performance analysis for the direct path link (non-cooperative link A-C) to establish the baseline performance as well as BER performance corresponding to the traditional BDF cooperative protocol analyzed in [19]. Here, it is assumed that the average optical power transmitted from each node is P_{opt}, being adopted an OOK signaling based on a constellation of two equiprobable points in a one-dimensional space with an Euclidean distance of $d_E = 2P_{\text{opt}}\sqrt{T_b\xi}$, where the parameter T_b is the bit period and ξ represents the square of the increment in Euclidean distance due to the use of a pulse shape of high PAOPR, as explained in a greater detail in [10, appendix]. According to Eq. (1), the statistical channel model corresponding to the A-B link assuming repetition coding with EGC during the first and second frames can be written as

$$Y_{AB} = \frac{1}{2}X(I_{AB_1} + I_{AB_2}) + Z_{AB_{EGC}}, \quad X \in \{0, d_E\}, \quad Z_{AB_{EGC}} \sim N(0, N_0) \tag{5}$$

The information is detected each bit period, combining with the same weight 2 noisy faded signals in a similar manner to a SIMO FSO scheme with EGC [23] and, this way, increasing the diversity order for the source-relay link. As shown in Table 1, since in the first phase of the cooperative protocol the node A transmits the same information to the nodes B and C and the fact that in the second phase transmits again this information overlapping with the third phase corresponding to the symmetric scheme, the division by 2 is considered so as to maintain the average optical power in the air at a constant level of P_{opt}, being transmitted by each laser an average optical power of $P_{\text{opt}}/2$. Assuming channel side information at the receiver, the conditional BER at the node B is given by

$$P_b^{AB}\left(E|\, I_{AB_T}\right) = Q\left(\sqrt{(d_E/2)^2 i^2/4N_0}\right) = Q\left(\sqrt{(\gamma/4)\xi i}\right) \tag{6}$$

where I_{AB_T} represents the sum of variates $I_{AB_T} = I_{AB_1} + I_{AB_2}$, $Q(\cdot)$ is the Gaussian-Q function defined as $Q(x) = \frac{1}{\sqrt{2\pi}}\int_x^\infty e^{-\frac{t^2}{2}}dt$ and $\gamma = P_{\text{opt}}^2 T_b/N_0$ represents the received electrical SNR in absence of turbulence when the classical rectangular pulse shape is adopted for OOK formats. Since the variates I_{AB_1} and I_{AB_2} are independent, knowing that the resulting PDF of their sum I_{AB_T} can be determined by using the moment generating function of their corresponding PDFs, obtained via single-sided Laplace and its inverse transforms, approximate expression for the PDF, $f_{I_{AB_T}}(i)$, of the combined variates can be easily derived from Eq. (4) as

$$f_{I_{AB_T}}(i) \approx \frac{a_{AB}^2 \Gamma(b_{AB})^2}{\Gamma(2b_{AB})} i^{2b_{AB}-1} e^{i \frac{2c_{AB} b_{AB} \Gamma(2b_{AB})}{a_{AB} \Gamma(2b_{AB}+1)}} \tag{7}$$

Hence, the average BER, $P_b^{AB}(E)$, can be obtained by averaging $P_b^{AB}\left(E|\, I_{AB_T}\right)$ over the PDF as follows

$$P_b^{AB}(E) = \int_0^\infty Q\left(\sqrt{(\gamma/4)\xi i}\right) f_{I_{AB_T}}(i) di. \tag{8}$$

To evaluate the integral in Eq. (8), we can use that the Q-function is related to the complementary error function $\text{erfc}(\cdot)$ by $\text{erfc}(x) = 2Q(\sqrt{2}x)$ [28, eqn. (6.287)] and [31, eqn. (2.85.5.2)], obtaining the corresponding approximation of average BER as can be seen in

$$\begin{aligned} P_b^{AB}(E) \approx & \sqrt{\pi} 2^{(b_{AB}-1)} \gamma^{-b_{AB}} \Gamma(b_{AB})^2 a_{AB}^2 \, {}_2\tilde{F}_2\left(b_{AB}, b_{AB}+\frac{1}{2}; \frac{1}{2}, b_{AB}+1; \frac{2c_{AB}^2}{a_{AB}^2 \gamma}\right) \\ & + \frac{\sqrt{\pi} \gamma^{\frac{1}{2}(-2b_{AB}-1)} \Gamma(b_{AB})^2}{2^{-\frac{1}{2}(2b_{AB}-1)} (a_{AB} b_{AB} c_{AB})^{-1}} \, {}_2\tilde{F}_2\left(b_{AB}+\frac{1}{2}, b_{AB}+1; \frac{3}{2}, b_{AB}+\frac{3}{2}; \frac{2c_{AB}^2}{a_{AB}^2 \gamma}\right). \end{aligned} \tag{9}$$

where ${}_p\tilde{F}_q(a_1, \cdots, a_p; b_1, \cdots, b_q; x)$ is the generalized hypergeometric function [28, eqn. (9.14.1)] and the value of the parameters a_{AB} and b_{AB} depends on the relation between φ^2 and β as obtained in Eq. (4). Considering now that the PDF in Eq. (2) is approximated by using the first term of the Taylor expansion, i.e. assuming in Eq. (9) a value of $c_{AB} = 0$, it is straightforward to show that the average BER behaves asymptotically as $(\Lambda_c \gamma \xi)^{-\Lambda_d}$, where Λ_d and Λ_c denote diversity order and coding gain, respectively. At high SNR, if asymptotically the error probability behaves as $(\Lambda_c \gamma \xi)^{-\Lambda_d}$, the diversity order Λ_d determines the slope of the BER versus average SNR curve in a log-log scale and the coding gain Λ_c (in decibels) determines the shift of the curve in SNR. Since $c_{AB} = 0$ we can use in Eq. (9) that ${}_pF_q\left(a_1, \ldots, a_p; b_1, \ldots, b_q; 0\right) = 1$ [28, eqn. (9.14.1)]. It is easy to deduce that $P_b^{AB}(E)$ behaves asymptotically as $1/\gamma^{b_{AB}}$, corroborating not only that the diversity order corresponding to the source-relay link is independent of the pointing error when $\varphi^2 > \beta$ but also the fact that the diversity order has been increased twice if compared to the BDF cooperative protocol analyzed in [19], as also shown in [20].

Once the error probability at the node B is known, two cases can be considered to evaluate the BER corresponding to the BDF cooperative protocol here proposed depending on the fact that the bit from the relay A-B-C is detected correctly or incorrectly. In this way, the statistical channel model corresponding to the BDF cooperative protocol, i.e. the bits received at C directly from A-C link and from the relay A-B-C can be written as

$$Y_{BDF} = \frac{1}{2} X I_{AC} + Z_{AC} + \frac{1}{2} X^* I_{BC} + Z_{BC}, \quad X \in \{0, d_E\}, \quad Z_{AC}, Z_{BC} \sim N(0, N_0/2) \tag{10}$$

where X^* represents the random variable corresponding to the information detected at the node B and, hence, $X^* = X$ when the bit has been detected correctly at B and $X^* = d_E - X$ when the bit has been detected incorrectly. As shown in Table 1, since in the first phase of the cooperative protocol the node A transmits the same information to the nodes B and C and the fact that the third phase is overlapped with the second phase corresponding to the symmetric scheme, transmitting information from node B to nodes C and A, the division by 2 is considered so as to maintain the average optical power in the air at a constant level of P_{opt}, being transmitted by each laser an average optical power of $P_{\text{opt}}/2$.

Considering that the bit is correctly detected at B, the statistical channel model for the BDF cooperative protocol can be expressed as

$$Y_{BDF_0} = \frac{1}{2} X \left(I_{AC} + I_{BC} \right) + Z_{BDF_{EGC}}, \quad X \in \{0, d_E\}, \quad Z_{BDF_{EGC}} \sim N(0, N_0) \tag{11}$$

As in previous analysis corresponding to the source-relay link, the conditional BER at the node C is given by $P_b^{BDF_0}\left(E | \, I_T \right) = Q\left(\sqrt{(\gamma/4)\xi i} \right)$, where I_T represents the sum of variates $I_T = I_{AC} + I_{BC}$. Since the variates I_{AC} and I_{BC} are independent, knowing that the resulting PDF of their sum I_T can be determined by using the moment generating function of their corresponding PDFs, obtained via single-sided Laplace and its inverse transforms, approximate expression for the PDF, $f_{I_T}(i)$, of the combined variates can be easily derived from Eq. (4) as

$$f_{I_T}(i) \approx \frac{a_{AC} a_{BC} \Gamma(b_{AC}) \Gamma(b_{BC})}{\Gamma(b_{AC} + b_{BC})} i^{b_{AC} + b_{BC} - 1} e^{i \frac{\Gamma(b_{AC} + b_{BC})(a_{AC} b_{BC} c_{BC} + a_{BC} b_{AC} c_{AC})}{a_{AC} a_{BC} \Gamma(b_{AC} + b_{BC} + 1)}}. \tag{12}$$

From this expression, the average BER, $P_b^{BDF_0}(E)$, can be determined as follows

$$P_b^{BDF_0}(E) = \int_0^\infty Q\left(\sqrt{(\gamma/4)\xi i} \right) f_{I_T}(i) di. \tag{13}$$

Evaluating this integral as in Eq. (8), we can obtain the corresponding closed-form asymptotic solution for the BER as follows

$$\begin{aligned}
&P_b^{BDF_0}(E) \approx \sqrt{\pi} 2^{\frac{1}{2}(b_{AC} + b_{BC} - 2)} a_{AC} a_{BC} \Gamma(b_{AC}) \Gamma(b_{BC}) \gamma^{-\frac{1}{2}(b_{AC} + b_{BC})} \\
&\times {}_2\tilde{F}_2\left(\frac{b_{AC} + b_{BC}}{2}, \frac{b_{AC} + b_{BC} + 1}{2}; \frac{1}{2}, \frac{b_{AC} + b_{BC} + 2}{2}; \frac{2(a_{BC} b_{AC} c_{AC} + a_{AC} b_{BC} c_{BC})^2}{a_{AC}^2 a_{BC}^2 (b_{AC} + b_{BC})^2 \gamma} \right) \\
&+ \sqrt{\pi} 2^{\frac{1}{2}(b_{AC} + b_{BC} - 2)} \Gamma(b_{AC}) \Gamma(b_{BC}) (a_{AC} b_{BC} c_{BC} + a_{BC} b_{AC} c_{AC}) \gamma^{-\frac{1}{2}(b_{AC} + b_{BC} + 1)} \\
&\times {}_2\tilde{F}_2\left(\frac{b_{AC} + b_{BC} + 1}{2}, \frac{b_{AC} + b_{BC} + 2}{2}; \frac{3}{2}, \frac{b_{AC} + b_{BC} + 3}{2}; \frac{2(a_{BC} b_{AC} c_{AC} + a_{AC} b_{BC} c_{BC})^2}{a_{AC}^2 a_{BC}^2 (b_{AC} + b_{BC})^2 \gamma} \right)
\end{aligned} \tag{14}$$

From this expression, as previously commented in Eq. (9), it is easy to deduce that $P_b^{BDF_0}(E)$ behaves asymptotically as $1/\gamma^{\frac{1}{2}(b_{AC}+b_{BC})}$ when $c_{AC}=0$ and $c_{BC}=0$ are considered, assuming now that the PDF in Eq. (2) is approximated by using only the first term of the Taylor expansion.

Alternatively, considering now that the bit is incorrectly detected at B, the statistical channel model for the BDF cooperative protocol can be expressed as

$$Y_{BDF_1} = \frac{1}{2} X\left(I_{AC} - I_{BC}\right) + \frac{d_E}{2} I_{BC} + Z_{BDF_{EGC}}, \quad X \in \{0, d_E\}, \quad Z_{BDF_{EGC}} \sim N(0, N_0) \tag{15}$$

Assuming channel side information at the receiver and given that the statistics corresponding to the term $\frac{d_E}{2} I_{BC}$ become irrelevant to the detection process, the conditional BER at the node C is given by $P_b^{BDF_1}\left(E \mid I_{AC}, I_{BC}\right) = Q\left(\sqrt{(\gamma/4)\xi}(i_1 - i_2)\right)$. Hence, the average BER, $P_b^{BDF_1}(E)$, can be obtained by averaging over the PDF as follows

$$P_b^{BDF_1}(E) = \int_0^\infty \int_0^\infty Q\left(\sqrt{(\gamma/4)\xi}(i_1 - i_2)\right) f_{I_{AC}}(i_1) f_{I_{BC}}(i_2) di_1 di_2. \tag{16}$$

Unfortunately, the result in Eq. (16) is not dominated by the behavior of the PDF near the origin because of the argument of the Gaussian-Q function is not always positive [32]. As in [19], to overcome this inconvenience, we can use the expression $Q(-x) = 1 - Q(x)$ to manipulate the negative values on the argument of the Gaussian-Q function in Eq. (16) together with the fact that Gaussian-Q function tends to 0 as $\gamma \to \infty$, simplifying the integral in Eq. (16) as follows

$$P_b^{BDF_1}(E) \doteq \int_0^\infty \int_0^{i_2} f_{I_{AC}}(i_1) f_{I_{BC}}(i_2) di_1 di_2. \tag{17}$$

It can be noted that the asymptotic behavior of $P_b^{BDF_1}(E)$ is independent of the SNR γ, resulting in a positive value that is upper bounded by 1. To evaluate the integral (17), we can use the Meijer's G-function [28, eqn. (9.301)], available in standard scientific software packages such as Mathematica and Maple, in order to transform the integral expression to the form in [33, eqn. (21)], expressing $K_\mu(\cdot)$ [33, eqn. (14)] in terms of Meijer's G-function. In this way, a closed-form solution is derived as can be seen in

$$P_b^{BDF_1}(E) \doteq \frac{\left(\varphi_{AC}^2 \varphi_{BC}^2\right) G_{5,5}^{3,4}\left(\frac{\zeta_{BC}\alpha_{AC}\beta_{AC}A_{0_{BC}}}{\zeta_{AC}\alpha_{BC}\beta_{BC}A_{0_{AC}}} \middle| \begin{matrix} 1, 1-\alpha_{BC}, 1-\beta_{BC}, 1-\varphi_{BC}^2, \varphi_{AC}^2+1 \\ \varphi_{AC}^2, \alpha_{AC}, \beta_{AC}, -\varphi_{BC}^2, 0 \end{matrix}\right)}{\Gamma(\alpha_{AC})\Gamma(\alpha_{BC})\Gamma(\beta_{AC})\Gamma(\beta_{BC})}. \tag{18}$$

Nonetheless, it must be emphasized that the Meijer's G-function has to be numerically calculated and, hence, the use of Monte Carlo integration to solve Eq. (17) may represent an alternative with less computational load. Once the error probability at the node B is known and considering these two cases, i.e. depending on the fact that the bit from the relay A-B-C is detected correctly or incorrectly, the BER corresponding to the BDF cooperative protocol here proposed is given by

$$P_b^{BDF}(E) = P_b^{BDF_0}(E) \cdot (1 - P_b^{AB}(E)) + P_b^{BDF_1}(E) \cdot P_b^{AB}(E). \tag{19}$$

This expression can be simplified taking into account the asymptotic behavior previously obtained in Eq. (9) and Eq. (14) as follows

$$P_b^{BDF}(E) \doteq P_b^{BDF_0}(E), \qquad b_{AC} + b_{BC} < 2b_{AB} \tag{20a}$$

$$P_b^{BDF}(E) \doteq P_b^{BDF_1}(E) \cdot P_b^{AB}(E), \qquad b_{AC} + b_{BC} > 2b_{AB} \tag{20b}$$

Taking into account these expressions, the adoption of the BDF cooperative protocol here analyzed translates into a diversity order gain, G_d, relative to the non-cooperative link A-C of

$$G_d = \min(b_{AC} + b_{BC}, 2b_{AB})/b_{AC} \tag{21}$$

Comparing with [19, eqn. (25)], it must be noted that a factor of 2 is included in relation to the diversity order depending on the source-relay link because of repetition coding assumed in the cooperative protocol based on time diversity, as was shown in [20] using alternative expressions. As shown in [11, 19] by the authors, it can be deduced that the main aspect to consider in order to optimize the error-rate performance is the relation between φ^2 and β, corroborating that the diversity order corresponding to each link is independent of the pointing error when $\varphi^2 > \beta$. Once this condition is satisfied an analysis about how Eq. (21) can be optimized is required, evaluating if the diversity order corresponding cooperative protocol is determined by the source-destination and relay-destination links or by the source-relay link. For the better understanding of the impact of the configuration of the three-node cooperative FSO system under study, the diversity order gain G_d in Eq. (21) as a function of the horizontal displacement of the relay node, x_B, is depicted in Fig. 2 for a source-destination link distance d_{AC}= {3 km, 6 km} and different turbulence conditions when different relay locations along the source-destination distance are assumed. Here, the diversity order gain corresponding to the BDF cooperative protocol analyzed in [19] is also included in order to show the improvement in performance achieved when repetition coding is assumed in the source-relay link transmission. In contrast to the analysis in [19], it must be commented that the impact of the deterministic propagation loss ζ_m is here considered, assuming clear weather conditions with visibility of 16 km. Here, the parameters α and β are calculated from Eq. ($3a$) and Eq. ($3b$), $\lambda = 1550$ nm and values of $C_n^2 = 1.7 \times 10^{-14}$ and $C_n^2 = 8 \times 10^{-14}$ $m^{-2/3}$ for moderate and strong turbulence, respectively, are adopted. In any case, the condition $\varphi^2 > \beta$ is satisfied for each link and, hence, these results are independent of pointing errors. These curves are corresponding to the intersection of two profiles related to the expressions $(\beta_{AC} + \beta_{BC})/\beta_{AC}$ and $2\beta_{AB}/\beta_{AC}$, as deduced from Eq.

(21). The improvement in performance can be easily corroborated by the fact that, even when the available diversity order is dependent on the relay location, this is now related to the expression $2\beta_{AB}/\beta_{AC}$, being twice as in [19], fully exploiting the potential time-diversity available in the turbulent channel corresponding to the source-relay link. It can be noted that a diversity order greater than two is always guaranteed regardless of the relay location and source-destination link.

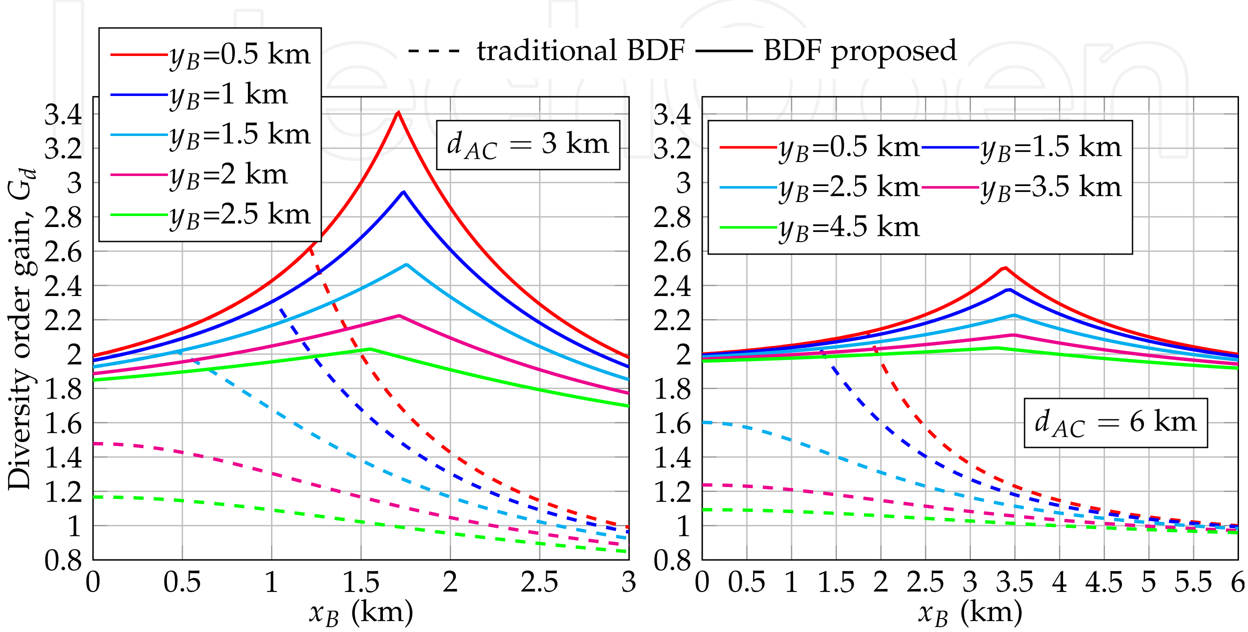

(a) Moderate turbulence ($C_n^2 = 1.7 \times 10^{-14}\ m^{-2/3}$)

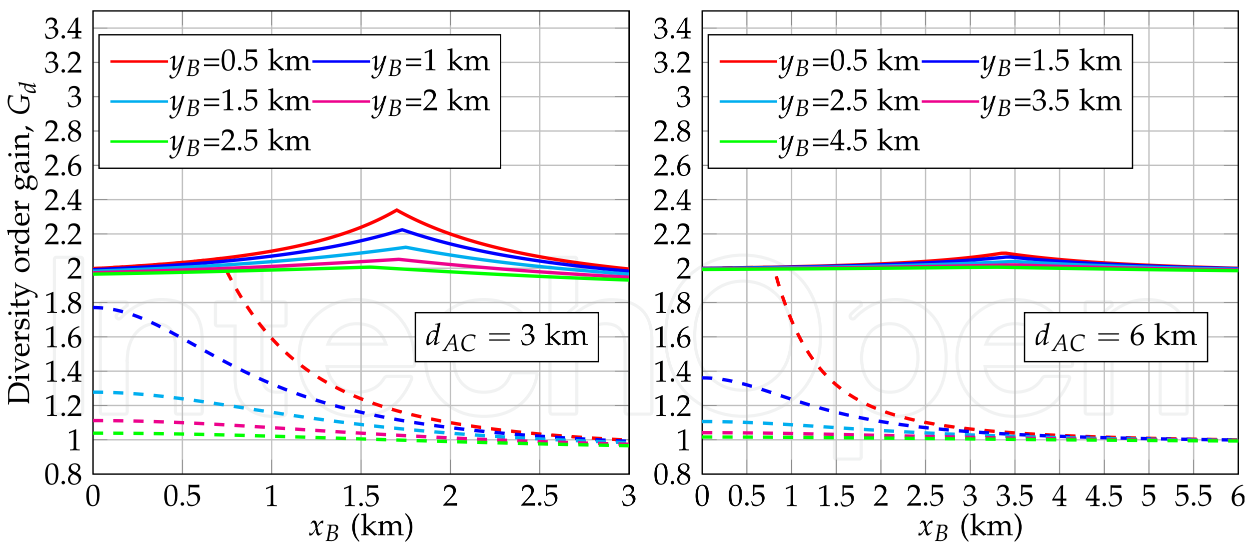

(b) Strong turbulence ($C_n^2 = 8 \times 10^{-14}\ m^{-2/3}$)

Figure 2. Diversity order gain for source-destination link distances of $d_{AC} = \{3, 6\}$ km when different relay locations are assumed.

The approximate BER results corresponding to this analysis with rectangular pulse shapes and $\xi = 1$ are illustrated in Fig. 3, when different relay locations for source-destination link distances d_{AC}= {3 km, 6 km} are assumed together with values of normalized beamwidth and normalized jitter of $(\omega_z/r, \sigma_s/r) = (5, 1)$ and $(\omega_z/r, \sigma_s/r) = (10, 2)$. Monte Carlo simulation results are furthermore included as a reference, confirming the accuracy and usefulness of the derived results. Due to the long simulation time involved, simulation results only up to BER=10^{-9} are included. Simulation results corroborate that approximate expressions here obtained lead to simple bounds on the bit error probability that get tighter over a wider range of SNR compared to asymptotic expressions previously presented in [20]. Additionally, we also consider the performance analysis for the direct path link (non-cooperative link A-C) to establish the baseline performance as well as BER performance corresponding to the BDF cooperative protocol analyzed in [19].

As expected, it can be corroborated that these BER results are in excellent agreement with previous results shown in Fig. 2 in relation to the diversity order gain achieved for this 3-way FSO communication setup. For the moderate turbulence case, diversity gains of 3.18 and 2.6 are achieved when d_{AC}=3 km and relay locations of (x_B=1.6 km; y_B=0.5 km) and (x_B=2 km; y_B=1 km), respectively, in contrast to the diversity gains of 1.84 and 1.3 achieved by the BDF cooperative protocol analyzed in [19]. Analogously, it can be seen that diversity gains of 2.07 and 2.18 are obtained when d_{AC}=6 km and relay locations of (x_B=2 km; y_B=2.5 km) and (x_B=4.5 km; y_B=0.5 km), respectively, in contrast to the diversity gains of 1.31 and 1.09 achieved by the BDF cooperative protocol analyzed in [19]. For the strong turbulence case, the improvement in diversity order gain is even more significant. From previous results, it can be concluded that not only a significant improvement in performance has been obtained by increasing the diversity order but also that a greater robustness is now achieved regardless of the source-destination link distance. As shown in Fig. 2, it can be deduced from Eq. (21) that the diversity order gain, G_d, is lower as the value of y_B is increased, presenting a maximum value wherein the two profiles related to the expressions $(\beta_{AC} + \beta_{BC})/\beta_{AC}$ and $2\beta_{AB}/\beta_{AC}$ intersect.

Additionally, a greater robustness to the impact of pointing errors is provided by the BDF cooperative protocol here proposed in case that the condition $\varphi^2 > \beta$ is not satisfied, as shown in Fig. 4 for a vertical displacement of the relay node of y_B=0.5 km and a source-destination link distance of d_{AC} = 3 km when moderate turbulence conditions are considered. In this configuration, a normalized beamwidth of $\omega_z/r = 7$ and different values of normalized jitter $\sigma_s/r = \{1, 2.5, 4\}$ are assumed in order to contrast the impact of pointing errors when the condition $\varphi^2 > \beta$ is or not satisfied for each link. It can be observed that diversity gains even greater than 3 are achieved by the BDF protocol here proposed when $(\omega_z/r, \sigma_s/r) = (7, 1)$, not being affected by pointing errors, decreasing this value down to 2 as the normalized jitter increases. However, a remarkably greater deterioration in performance is displayed when the traditional BDF protocol is considered.

These conclusions are contrasted in Fig. 5, wherein BER performance for a source-destination link distance of $d_{AC} = 3$ km and a relay location of (x_B=1.7 km; y_B=0.5 km) when values of normalized beamwidth of $\omega_z/r = 7$ and normalized jitter of $\sigma_s/r = \{1, 2.5, 4\}$ are assumed. As before, we also consider the performance analysis for the direct path link (non-cooperative link A-C) to establish the baseline performance. These BER results are in excellent agreement with previous results shown in Fig. 4 in relation to the diversity order gain achieved for this 3-way FSO communication setup when pointing errors are present. In this way, diversity gains of 3.4, 2.3 and 2 are achieved when values of normalized jitter of $\sigma_s/r = \{1, 2.5, 4\}$ are assumed, respectively.

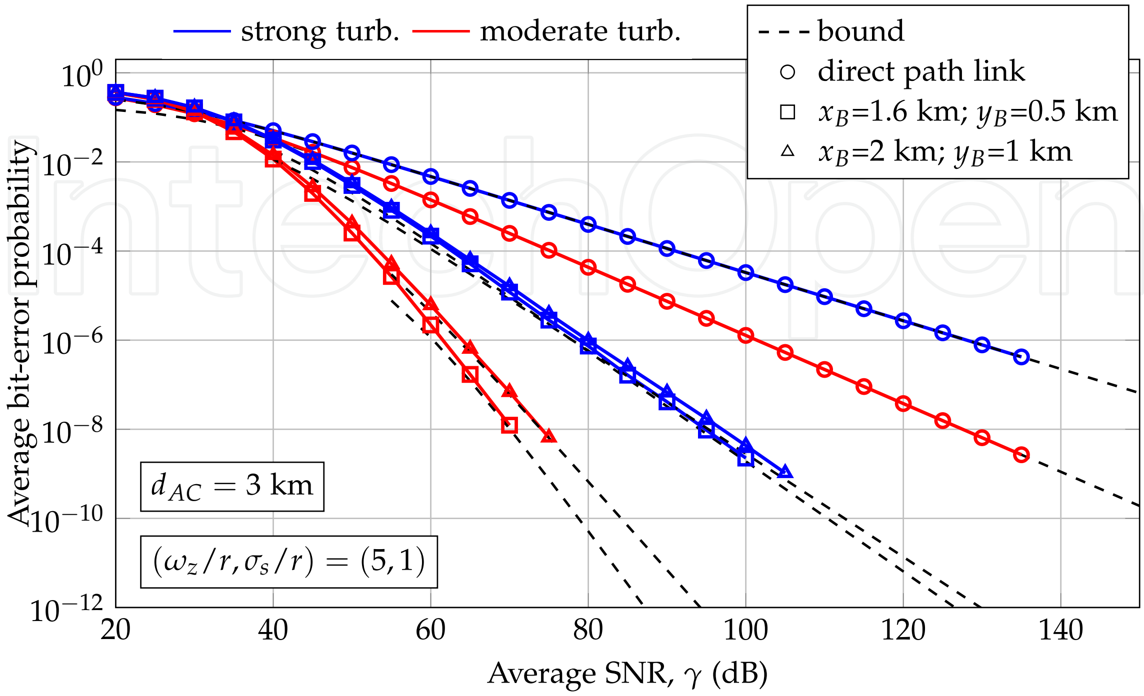

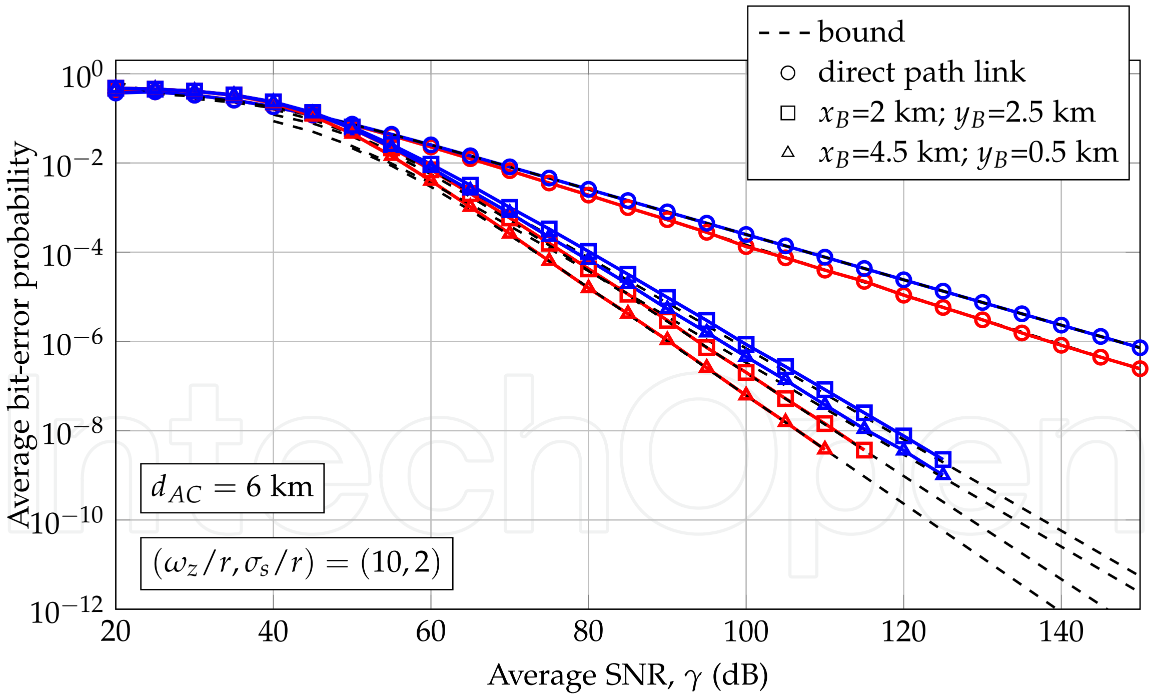

Figure 3. BER performance when different relay locations for $d_{AC} = \{3, 6\}$ km are assumed together with values of normalized beamwidth and normalized jitter of $(\omega_z/r, \sigma_s/r) = (5, 1)$ and $(\omega_z/r, \sigma_s/r) = (10, 2)$, respectively, and moderate and strong turbulence conditions are considered.

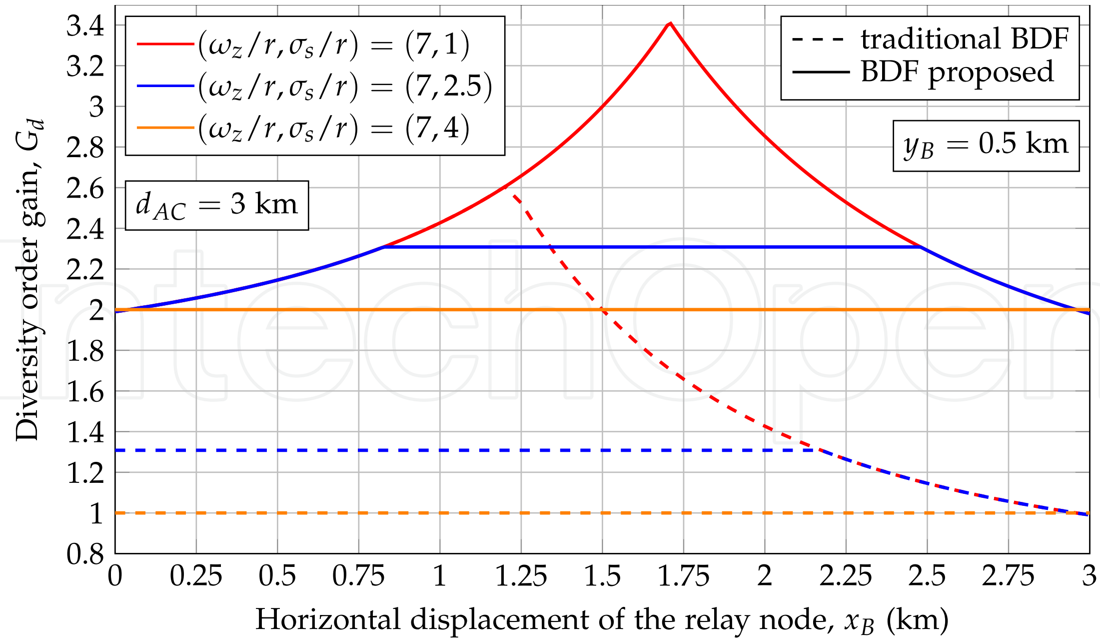

Figure 4. Diversity order gain G_d for a source-destination link distance of $d_{AC} = 3$ km and vertical displacement of the relay node of $y_B = 0.5$ km when moderate turbulence conditions, values of normalized beamwidth of $\omega_z/r = 7$ and normalized jitter of $\sigma_s/r = \{1, 2.5, 4\}$ are assumed.

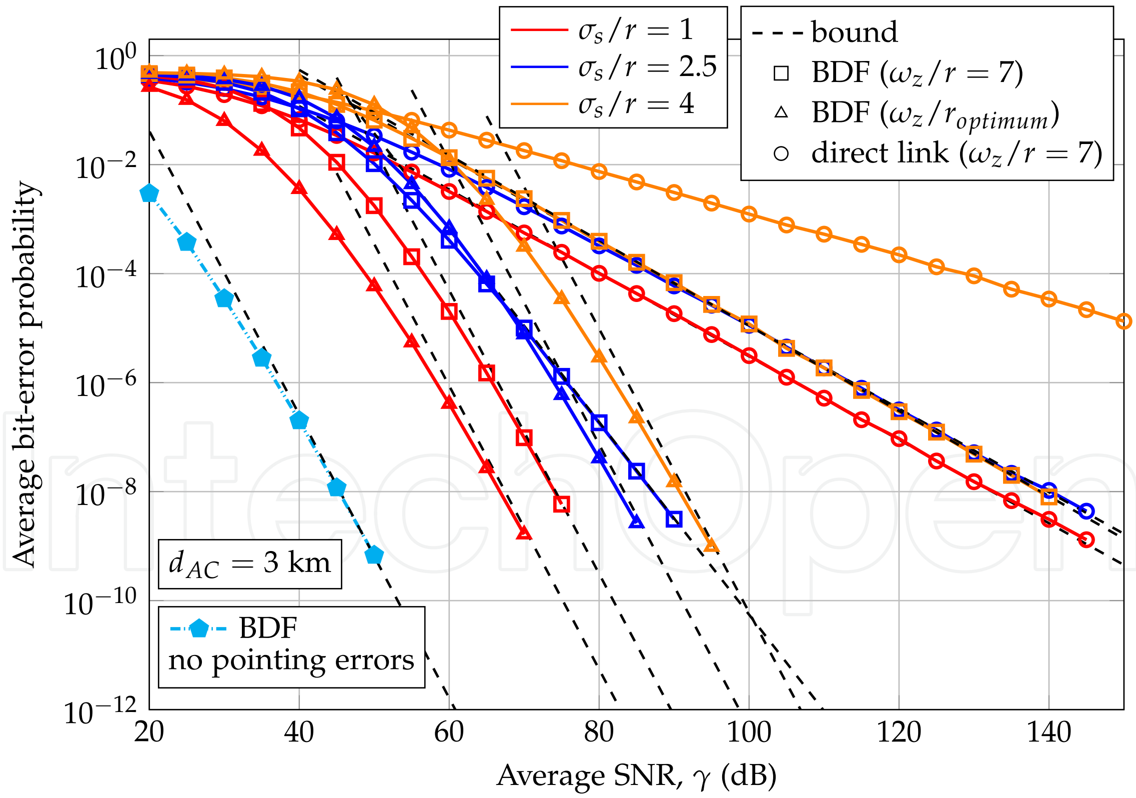

Figure 5. BER performance is depicted for $d_{AC} = 3$ km and a relay location of (x_B=1.7 km; y_B=0.5 km) when values of $\omega_z/r = 7$ and $\sigma_s/r = \{1, 2.5, 4\}$ are assumed as well as when no pointing errors are considered. Results assuming the optimum beamwidth corresponding to these values of normalized jitter are also included.

As concluded in [11, 19] by the authors, the adoption of transmitters with accurate control of their beamwidth is especially important to satisfy the condition $\varphi^2 > \beta$ in order to maximize the diversity order gain. Once this condition is satisfied, it can be convenient to compare with the BER performance obtained in a similar context when misalignment fading is not present. Knowing that the impact of pointing errors in our analysis can be suppressed by assuming $A_0 \to 1$ and $\varphi^2 \to \infty$ [7], the corresponding asymptotic expression for the configuration analyzed in Fig. 4 can be easily derived from Eq. $(20a)$ as follows

$$P_b^{BDF}(E) \doteq \frac{a_{AC}^{npe} a_{BC}^{npe} 2^{\frac{\beta_{AC}+\beta_{BC}}{2}} \Gamma(\beta_{AC})\Gamma(\beta_{BC})}{2L_{AC}^{\beta_{AC}} L_{BC}^{\beta_{BC}} \Gamma\left(\frac{1}{2}(\beta_{AC}+\beta_{BC}+2)\right)} (\gamma\xi)^{-\frac{1}{2}(\beta_{AC}+\beta_{BC})}, \tag{22}$$

where the parameters a_{AC}^{npe} and a_{BC}^{npe} are obtained from the Taylor expansion in Eq. (4) when no pointing errors are present as follows

$$a_m^{npe} = \frac{(\alpha_m\beta_m)^{\beta_m}\Gamma(\alpha_m-\beta_m)}{\Gamma(\alpha_m)\Gamma(\beta_m)}. \tag{23}$$

In Fig. 5, BER performance in the same FSO context without pointing errors is also displayed. In the same way as concluded in [19], the impact of the pointing error effects translates into a coding gain disadvantage, $D_{pe}[dB]$, relative to this 3-way FSO communication setup without misalignment fading given by

$$D_{pe}[dB] \triangleq \frac{20}{\beta_{AC}+\beta_{BC}} \log_{10}\left(\frac{\varphi_{AC}^2}{A_{0_{AC}}^{\beta_{AC}}(\varphi_{AC}^2-\beta_{AC})} \frac{\varphi_{BC}^2}{A_{0_{BC}}^{\beta_{BC}}(\varphi_{BC}^2-\beta_{BC})}\right). \tag{24}$$

According to this expression, it can be observed in Fig. 5 that a coding gain disadvantage of 28.75 decibels is achieved for a value of $(\omega_z/r, \sigma_s/r) = (7,1)$ in the three-node cooperative FSO system here proposed. Since proper FSO transmission requires transmitters with accurate control of their beamwidth, the optimization procedure is finished by finding the optimum beamwidth, ω_z/r, that gives the minimum BER performance. It can be observed that this is equivalent to minimize the expression in Eq. (24), deducing that the optimization process for the transmit laser corresponding to the source node and the optimization process corresponding to the relay node are independent. Hence, the optimum beamwidth for each transmit laser can be achieved using numerical optimization methods for different values of normalized jitter, σ_s/r and turbulence conditions [34] in a similar approach as reported in [11]. In this way, it can be shown that BER optimization provides numerical results for the normalized beamwidth ω_z/r following a linear performance for each value of distance, where its corresponding slope is subject to the turbulence conditions. This leads to easily obtain a first-degree polynomial given by

$$\omega_z/r_{optimum} \approx \left(-0.034\beta^2 + 0.72\beta + 2.15\right)\sigma_s/r, \tag{25}$$

where the slope follows a quadratic form in β [11]. The use of this expression is also shown in Fig. 5, where results assuming the optimum beamwidth corresponding to values of normalized jitter of $\sigma_s/r = \{1, 2.5, 4\}$ are also included. Using Eq. (25) for a value of $\sigma_s/r = 1$, a coding gain disadvantage of $D_{pe} = 21.6$ decibels is achieved when values of $\omega_z/r_{AC} = 3.17$ and $\omega_z/r_{BC} = 4.17$ are assumed, improving BER performance in 7 decibels if compared to previous case wherein $\omega_z/r = 7$ is considered for source-destination and relay-destinations links. Additionally, an even greater improvement in BER performance is corroborated for values of normalized jitter of 2.5 and 4, wherein the diversity order is increased since the condition $\varphi^2 > \beta$ is satisfied. In this way, using Eq. (25) for a value of $\sigma_s/r = 2.5$, a coding gain disadvantage of $D_{pe} = 37.49$ decibels is achieved when values of $\omega_z/r_{AC} = 7.93$ and $\omega_z/r_{BC} = 10.43$ are assumed. Using Eq. (25) for a value of $\sigma_s/r = 4$, values of $\omega_z/r_{AC} = 12.68$ and $\omega_z/r_{BC} = 16.69$ are obtained, achieving a coding gain disadvantage of $D_{pe} = 45.65$ decibels relative to this 3-way FSO communication setup without misalignment fading. Nonetheless, it must be emphasized in this case that nearly 50 decibels less in average SNR are required to guarantee a target BER of 10^{-8} after optimizing the normalized beamwidth ω_z/r.

4. Conclusions

In this chapter, a novel closed-form approximation bit error-rate (BER) expression based on [21] is presented for a 3-way FSO communication setup when the irradiance of the transmitted optical beam is susceptible to either a wide range of turbulence conditions (weak to strong), following a gamma-gamma distribution of parameters α and β, or pointing errors, following a misalignment fading model where the effect of beam width, detector size and jitter variance is considered. The resulting BER expression is shown to be very accurate in the range from low to high SNR, requiring the first two terms of the Taylor expansion of the channel probability density function (PDF). Simulation results are further demonstrated to confirm the accuracy and usefulness of the derived results. Fully exploiting the potential time-diversity available in the turbulent channel, a greater diversity gain determined by $G_d = \min(\beta_{AC} + \beta_{BC}, 2\beta_{AB})/\beta_{AC}$ is achieved, where β_{AC}, β_{BC} and β_{AB} are parameters corresponding to the turbulence of the source-destination, relay-destination and source-relay links. The superiority of the BDF relaying scheme using time diversity, compared with the traditional cooperative protocol, is corroborated by the obtained results since a greater robustness is provided not only to the pointing errors but also to the relay location, presenting a similar performance regardless of the source-destination link distance. Additionally, asymptotic expressions are used to find the optimum beamwidth that minimizes the BER at different turbulence conditions as well as to determine a more favorable relay location.

Acknowledgments

The authors wish to acknowledge the financial support given by the Spanish MINECO Project TEC2012-32606.

http://dx.doi.org/10.5772/58996

Author details

Rubén Boluda-Ruiz[1], Beatriz Castillo-Vázquez[1], Carmen Castillo-Vázquez[2], and Antonio García-Zambrana[1]

1 Department of Communications Engineering, University of Málaga, Spain

2 Department of Statistics and Operations Research, University of Málaga, Málaga, Spain

References

[1] V. W. S. Chan. Free-space optical communications. *J. Lightwave Technol.*, 24(12):4750–4762, 2006.

[2] L.C. Andrews, R.L. Phillips, and C.Y. Hopen. *Laser beam scintillation with applications*. Bellingham, 2001.

[3] E. J. Lee and V. W. S. Chan. Part 1: optical communication over the clear turbulent atmospheric channel using diversity. *IEEE J. Sel. Areas Commun.*, 22(9):1896–1906, 2004.

[4] Ivan B. Djordjevic, Stojan Denic, Jaime Anguita, Bane Vasic, and MarkA. Neifeld. Ldpc-coded mimo optical communication over the atmospheric turbulence channel. *J. Lightwave Technol.*, 26(5):478–487, 2008.

[5] E. Bayaki, R. Schober, and R. K. Mallik. Performance analysis of mimo free-space optical systems in gamma-gamma fading. *IEEE Trans. Commun.*, 57(11):3415–3424, 2009.

[6] Antonio García-Zambrana, Carmen Castillo-Vázquez, and Beatriz Castillo-Vázquez. Space-time trellis coding with transmit laser selection for FSO links over strong atmospheric turbulence channels. *Opt. Express*, 18(6):5356–5366, 2010.

[7] A. A. Farid and S. Hranilovic. Outage capacity optimization for free-space optical links with pointing errors. *J. Lightwave Technol.*, 25(7):1702–1710, July 2007.

[8] H. G. Sandalidis, T. A. Tsiftsis, and G. K. Karagiannidis. Optical wireless communications with heterodyne detection over turbulence channels with pointing errors. *J. Lightwave Technol.*, 27(20):4440–4445, 2009.

[9] W. Gappmair, S. Hranilovic, and E. Leitgeb. Performance of ppm on terrestrial fso links with turbulence and pointing errors. *IEEE Commun. Lett.*, 14(5):468–470, 2010.

[10] Antonio García-Zambrana, Carmen Castillo-Vázquez, and Beatriz Castillo-Vázquez. Outage performance of MIMO FSO links over strong turbulence and misalignment fading channels. *Opt. Express*, 19(14):13480–13496, Jul 2011.

[11] Antonio García-Zambrana, Beatriz Castillo-Vázquez, and Carmen Castillo-Vázquez. Asymptotic error-rate analysis of fso links using transmit laser selection over gamma-gamma atmospheric turbulence channels with pointing errors. *Opt. Express*, 20(3):2096–2109, Jan 2012.

[12] A. Sendonaris, E. Erkip, and B. Aazhang. User cooperation diversity. part i. system description. *IEEE Trans. Commun.*, 51(11):1927 – 1938, nov. 2003.

[13] M. Safari and M. Uysal. Relay-assisted free-space optical communication. *IEEE Trans. Wireless Commun.*, 7(12):5441–5449, December 2008.

[14] M. Karimi and M. Nasiri-Kenari. Ber analysis of cooperative systems in free-space optical networks. *J. Lightwave Technol.*, 27(24):5639 –5647, dec.15, 2009.

[15] M. Karimi and M. Nasiri-Kenari. Outage analysis of relay-assisted free-space optical communications. *IET Communications*, 4(12):1423 –1432, 13 2010.

[16] C. Abou-Rjeily and A. Slim. Cooperative diversity for free-space optical communications: transceiver design and performance analysis. *IEEE Trans. Commun.*, 59(3):658 –663, march 2011.

[17] C. Abou-Rjeily and S. Haddad. Cooperative fso systems: performance analysis and optimal power allocation. *J. Lightwave Technol.*, 29(7):1058 –1065, april1, 2011.

[18] M.R. Bhatnagar. Performance analysis of decode-and-forward relaying in gamma-gamma fading channels. *IEEE Photon. Technol. Lett.*, 24(7):545 –547, april1, 2012.

[19] Antonio García-Zambrana, Carmen Castillo-Vázquez, Beatriz Castillo-Vázquez, and Rubén Boluda-Ruiz. Bit detect and forward relaying for fso links using equal gain combining over gamma-gamma atmospheric turbulence channels with pointing errors. *Opt. Express*, 20(15):16394–16409, Jul 2012.

[20] Antonio García-Zambrana, Carmen Castillo-Vázquez, and Beatriz Castillo-Vázquez. Improved BDF relaying scheme using time diversity over atmospheric turbulence and misalignment fading channels. *The Scientific World Journal*, 2014, 2014.

[21] Y. Dhungana and C. Tellambura. New simple approximations for error probability and outage in fading. *Communications Letters, IEEE*, 16(11):1760–1763, November 2012.

[22] Antonio García-Zambrana, Carmen Castillo-Vázquez, and Beatriz Castillo-Vázquez. Rate-adaptive FSO links over atmospheric turbulence channels by jointly using repetition coding and silence periods. *Opt. Express*, 18(24):25422–25440, Nov 2010.

[23] T. A. Tsiftsis, H. G. Sandalidis, G. K. Karagiannidis, and M. Uysal. Optical wireless links with spatial diversity over strong atmospheric turbulence channels. *IEEE Trans. Wireless Commun.*, 8(2):951–957, Feb. 2009.

[24] H. E. Nistazakis, E. A. Karagianni, A. D. Tsigopoulos, M. E. Fafalios, and G. S. Tombras. Average capacity of optical wireless communication systems over atmospheric turbulence channels. *IEEE/OSA Journal of Lightwave Technology*, 27(8):974–979, April15, 2009.

[25] Fang Xu, Ali Khalighi, Patrice Caussé, and Salah Bourennane. Channel coding and time-diversity for optical wireless links. *Opt. Express*, 17(2):872–887, 2009.

[26] C. H. Kwok, R. V. Penty, and I. H. White. Link reliability improvement for optical wireless communication systems with temporal-domain diversity reception. *IEEE Photon. Technol. Lett.*, 20(9):700–702, 2008.

[27] Isaac I. Kim, Bruce McArthur, and Eric J. Korevaar. Comparison of laser beam propagation at 785 nm and 1550 nm in fog and haze for optical wireless communications. In *Proc. SPIE 4214, Optical Wireless Communications III*, February 6 2001.

[28] I. S. Gradshteyn and I. M. Ryzhik. *Table of integrals, series and products*. Academic Press Inc., 7th edition, 2007.

[29] M. A. Al-Habash, L. C. Andrews, and R. L. Phillips. Mathematical model for the irradiance probability density function of a laser beam propagating through turbulent media. *Opt. Eng.*, 40:8, 2001.

[30] Ning Wang and Julian Cheng. Moment-based estimation for the shape parameters of the gamma-gamma atmospheric turbulence model. *Opt. Express*, 18(12):12824–12831, Jun 2010.

[31] A. P. Prudnikov, Yu Brychkov, and O. I. Marichev. *Integrals and Series. Volume 2: Special functions.*, volume 2. Gordon and Breach Science Publishers, 1986.

[32] Zhengdao Wang and G. B. Giannakis. A simple and general parameterization quantifying performance in fading channels. *IEEE Trans. Commun.*, 51(8):1389–1398, 2003.

[33] V. S. Adamchik and O. I. Marichev. The algorithm for calculating integrals of hypergeometric type functions and its realization in REDUCE system. In *Proc. Int. Conf. on Symbolic and Algebraic Computation*, pages 212–224, Tokyo, Japan, 1990.

[34] Wolfram Research, Inc. *Mathematica*. Wolfram Research, Inc., Champaign, Illinois, version 8.0.1. edition, 2011.

IntechOpen